Application of superposition method to study the mechanical behaviour of overlying strata in longwall mining

Songtao Ji [a,*], Hu He [b], Jurij Karlovšek [a]

[a] Geotechnical Engineering Centre, School of Civil Engineering, The University of Queensland, Brisbane 4067, Australia
[b] School of Resources and Geosciences, China University of Mining and Technology, Xuzhou, 221116, China

A R T I C L E   I N F O

A B S T R A C T

The sudden failure of roof strata is one of the fiercest dynamic instability events in underground longwall mining. To understand the mechanical behaviour of strata, researchers simplified the strata as a beam over an elastic foundation. However, some reported models involved a big equation system with unknown constants of integration. Solving such equations is a complicated mathematical task. As an improvement, this study adopted the superposition method to avoid arduous mathematical processes. In addition, the partially yielded coal seam and non-uniformly distributed overburden pressure were both considered in the proposed model. A set of case studies were carried out to investigate the influence of support scheme and yielded coal seam on strata behaviour. Results suggested the partially yielded coal seam is an essential condition to reproduce a reasonable strata behaviour. The strata can fail in front of the working face or over goaf controlled by the yield distance and yield degree of the coal seam. The bending moment and strain energy density are significantly reduced by increasing the yield distance and support capacity rather than yield degree. In addition to the above, results such as the deflection, slope, bending moment, shear force and strain energy density of strata and bearing pressure of coal seam were presented. This study demonstrated the superposition method is an easy tool to solve the mechanical model of overlying strata. By adopting this model, the failure patterns and mechanical state of overlying strata in longwall mining can be analytically investigated.

1. Introduction

The movement, fracturing and caving processes of roof strata are the primary concerns of underground longwall mining.[1] Hard roof, usually stronger and thicker sandstone, plays a controlling factor in overburden strata.[2,3] The collapse of a hard roof can cause a strong loading to the coal seam as well as its face support. Such a dynamic strong loading is one of the contributors to an occurrence of coal burst, and coal- and gas-outburst.[4] The prerequisite knowledge and learning of dynamic loading is understanding the failure mechanism of hard roof strata and its control factors. Therefore, it is necessary to have a detailed understanding of the mechanical state of the strata.

For more than a century, numerous models were proposed to explore the behaviour of roof strata induced by the mining operation. At the earlier stage, European researchers made an enormous contribution that laid the foundation for modern mining.[5–7]

In the literature, the earliest documented investigations of mining-induced strata deformation on mainland Europe, which also proposed the first formula to calculate the subsidence, were undertaken in Liège coalfield in Belgium, by Dumont[8] in 1871. In 1885, Fayol,[9] a French mine engineer and director, discovered the arching phenomenon (also known as dome theory) by adopting a stack of wood beams spanning simple support. This research suggested the strata tend to separate upon deflection and transfer the gravitational loading to abutments. Fayol's work on dome theory had great influence in the 1890s and for many years after.[7] In 1928, Jones and Davies[10] researched the pillar and stall working under a sandstone roof, based on the observation made upon the South Wales coalfield. This is a study of the behaviour of the strata consequence upon the extraction of coal that covers the seam, floor, roof and method of working, which was recognized as the first rigorous analysis of roof strata based on arching principles.[11] In 1929, Briggs[12] contributed greatly to an overall understanding of mining-induced subsidence. His summation of European experience was widely practised in the US and has been well-reviewed in literature.[5,13] Those researches conducted in early Europe laid the foundation for the modern understanding of ground movement and initiated theoretical studies of

---

* Corresponding author.
E-mail addresses: songtao.ji@uq.edu.au (S. Ji), hehu@cumt.edu.cn (H. He), j.karlovsek@uq.edu.au (J. Karlovšek).

strata control in world coal mining industry practice.

Since the 1950s, extensively researches were carried out to study the mining-induced strata movement by elastic theory. In 1957, King and Whetton[14] explained the ground movement by adopting the elastic theory that provides a fairly close agreement with a physical model experiment. Their work probably is the initial attempt to interpret the strata movement by elastic analysis. Hackett[15] investigated the ground displacement over a thin horizontal tabular deposit in the homogenous isotropic ground by considering the vertical direct stress around an excavation to be linearly increasing with depth and the vertical and horizontal direction stresses being equal.[16,17] 1960–1962, Berry and Sales[18–20] reported analytical researches that application of classical elastic theory to study the strata mechanical behaviour by isotropic treatment of the problem. Salamon[21–23] conducted a series of work that put forward ideas on elastic analysis of displacement and stresses of roof strata. He had discussed homogeneous, isotropic and transversely isotropic models and proposed the frictionless laminated model and multi-membrane model. Whittaker and Breeds[13] published a book that presented a comprehensive review of mining subsidence. In their study, the roof beam maximum tensile stress does not exceed the tensile strength of the roof beam is the criterion to assess the roof stability. Please et al.[24] taken the roof stratum as a clamped beam and examined the roof behaviour using a simple strut and beam theory. However, this model does not apply to situations where joint dip at less than about 75° as the shear failure prevents the generation of an arch.[25] Those works had been detailed reviewed by Kapp,[16] Donnelly,[5] Brady and Brown,[26] Kratzsch[27] and Peng[28]

Voussoir beam as one of the most widely used models for roof beam stability assessment is established by Evans[29] by using the analogy with the voussoir arch considered in masonry structures. Evans's theory was pioneering but had some inherent errors in the static that has been modified by Beer and Meek.[30] Subsequently, Brady and Brown,[26] Sofianos[6] and Diederichs and Kaiser[31] had made their contributions to the voussoir beam model. Brady and Brown[26] gave comprehensive reviews of the voussoir beam model. In China, two textbooks on strata control appeared in the 1980s, namely Qian[32] and Song.[33] Both books give a detailed instruction on the roof beam model and the application in coal mine design that greatly contributed to China's coal industry. The latest researches in terms of the voussoir beam model focus on how the thickness and shape of the compression arch are determined,[34] horizontal loading and its impact on the voussoir structure,[35] the rotational motions of the voussoir beam structures,[36] the formation condition of a voussoir beam[37] and application of voussoir beam in mining practice.[38,39] Those models contribute to a better understanding of the strata behaviour, however, concerning the dynamic disasters prediction and control, those models cannot depict the failure and strain energy evolution of strata in a precise way.

To explore a more accurate analytical model for roof strata, control factors such as the elastic foundation and non-uniformly distributed ground pressure must be addressed. Jiang and Jiang[40] described the roof strata as a clamped beam over an elastic foundation which exposed a better agreement with field-monitored data than the rigid foundation. Pan et al.[41,42] derived the expression of beam deflection by solving a system of differential equations for statically indeterminate structure. Yang et al.[43] adopted the cantilever beam over an elastic foundation to develop a roof failure analytical model. Zhang et al.[44] proposed a semi-analytical way that divided the hard roof into finite elements and adopted the analytical solution developed by Froio and Rizzi[45] to solve the mechanical behaviours of a hard roof approximately. The research is ongoing by various studies[46–49] trying to employ numerous models of the beam over elastic foundation to solve the mechanical behaviours of roof strata.

Those researches improved the model's accuracy significantly, however, the limitations of preceding studies in terms of oversimplified conditions and complex mathematics solutions are not well addressed. Some of these models ignored the partially yielded coal seam in front of

the working face, roof support and the overburden pressure which are the very essential factors to control the strata. From a mathematical point of view, for instance, in some studies,[41,42] the application of boundary, the equilibrium and the continuity conditions lead to an extensive system of equations. The solution is composed of general and particular solutions with constants of integration as unknowns. As suggested by Dinev,[50] the disadvantage of this method is complicated mathematics. Moreover, the plastic of the coal seam was represented by an artificially defined supporting force, in which, the control parameters need to be adjusted manually.

Due to the above weaknesses, the method of superposition is a more promising candidate to avoid these impediments. The method of superposition for beam over elastic foundation was developed over half a century ago.[51] The superposition method uses solutions of simple problems of infinitely long beams with different simple loads to construct the solution for the complex beam structure with types of loads and supports.[50] For the concise mathematical solution of the superposition method, it is a more general and easy-to-use approach to study the strata behaviour in underground mining.

The contribution of this study to the current knowledge is shown in Fig. 1. Researches[52–54] suggested the coal burst occurrences are affected by the combination of static stress σ_s and dynamic stress σ_d concentrations. In this study, the bearing pressure of the coal seam (static source), as well as the strain energy density of hard strata (dynamic source), will be solved analytically. Therefore, the location and magnitude of released dynamic energy as well as the distribution of static stress can be quantified.

In this study, control factors, such as non-uniformly distributed overburden pressure, roof support and partially yielded coal seam, were introduced into the analytical model. The deflection, bending moment, slope, shear force, strain energy density, tensile stress, and tensile strain of strata can be derived from the proposed method. In addition, the bearing pressure over unmined coal seam is also presented. A set of case studies were carried out to investigate the potential failure position of hard roof strata and its control factors. Further improvement of this model is also suggested at the end.

2. The mechanical model of overlying strata

2.1. The structure of overlying strata in longwall mining

The structure of overlying strata is extremely complex, (folds, faults, the various strata thickness, lithology, etc). Therefore, the failure characteristic of strata varies from one site to another. To have an overall understanding of strata movement, most studies simplify the overlying strata to an ideal scenario, one of the most commonly used simplified models is shown in Fig. 2.[55,56] The span distance of overlying strata keeps growing along with the retreat of a coal seam. When strata reach the ultimate strength, the first weighting occurs. The idealized caving
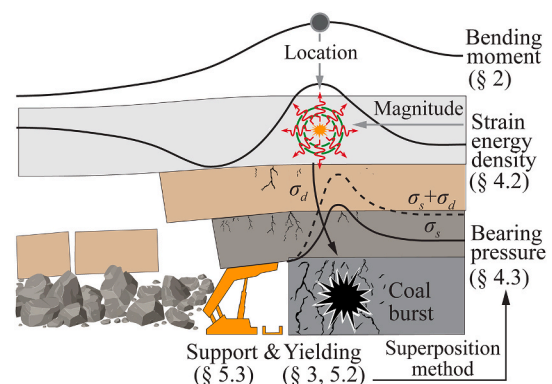

Fig. 1. Proposed method and its application in practice (after Dou et al.[53]).
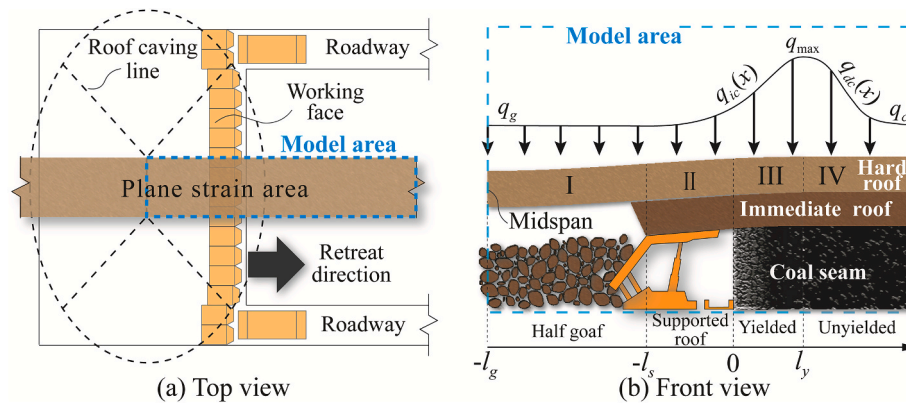
Fig. 2. Mechanical structure of overlying strata.

configuration is denoted by the roof caving line in Fig. 2a.

According to the plate and shell mechanics theory, the plane strain area of overlying strata (brown shaded area in Fig. 2a) at the middle of the longwall panel could be regarded as a plane strain mechanical model when considering its structure change in the retreat direction. Therefore, the unit width of hard roof strata, within the plane strain area, can be simplified as a beam structure. Before initial weighting, the strata beam with various boundaries, foundations and load conditions are displayed in Fig. 2b.

According to foundation conditions, the strata beam was divided into 4 beam segments, labelled from I to IV. Among which, l_g is the half distance of goaf, l_s is the roof support distance, l_y is the distance of yielded coal seam. The roof support distance l_s refers to the length of the residual immediate roof over excavated space that offers support resistance to the hard roof. l_s can be equal to or larger than the roof control distance. The roof control distance refers to the canopy length and distance of canopy tip-to-face. For instance, in Fig. 1, l_s is the length of suspended residual immediate roof that is larger than the roof control distance, whereas in Fig. 2, l_s is equal to the roof control distance as the immediate roof is fully supported by face supports. In practice, l_s can be measured in the field. In this study, l_s is equal to the roof control distance under an assumption that the immediate roof is fully caved as shown in Fig. 2b.

To improve the accuracy of this analytical model, the non-uniformly distributed overburden pressure and the yielded coal seam were taken into consideration. Segment-I is a beam over goaf without foundation support, segment-II is a beam over working face supported by face support, segment-III is a beam over partially yielded coal seam, and segment-IV is a beam over an un-yielded coal seam. In the following section, the non-uniformly distributed overburden pressure and the mechanical model with corresponding boundary conditions of each segment are introduced.

2.2. Typical non-uniformly distributed overburden pressure

The non-uniformly distributed overburden pressure is a very important factor when investigating rockburst related behaviour. The increased overburden pressure rapidly increases with distance into the yielded zone in the coal seam, producing peak stress with 4–5 times of the overburden stress, meanwhile, a large amount of elastic energy is stored in un-yielded surrounding rock mass.[57,58] Therefore, it is necessary to have a full consideration of non-uniformly distributed overburden pressure in the proposed analytical model. Wilson[59] proposed a calculation method of the non-uniformly distributed overburden pressure based on the stress balance method in which the total vertical force applied over the foundation is equal to that caused by the overburden. A

Weibull function was suggested to represent non-uniformly distributed overburden pressure to derive the equation for beam deflection.[41]

In this study, the expression of non-uniformly distributed overburden pressure is satisfied with continuous conditions of corresponding intersections of beams. Moreover, as higher-order derivatives are involved, the exponential expression of non-uniformly distributed overburden pressure is expected to simplify the calculation (the derivative of e^x with respect to x is equal to e^x itself, without increase the expression complexity). Based on the previous study[41] the expression of non-uniformly distributed overburden pressure are expressed as

$$\begin{cases} q_{ic}(x) = q_g + \dfrac{q_{max}e}{l_{ic}}\left(-x + l_y + l_{ic}\right)e^{\frac{x-l_y-l_{ic}}{l_{ic}}} & \left(-l_g \leq x \leq l_y\right) \\[2mm] q_{dc}(x) = q_c + \dfrac{(q_{max}+q_g-q_c)e}{l_{dc}}\left(x - l_y + l_{dc}\right)e^{\frac{-x+l_y-l_{dc}}{l_{dc}}} & \left(l_y < x\right) \end{cases}$$

(1)

where $q_{ic}(x)$ is the rising overburden pressure, $q_{dc}(x)$ is the decreased overburden pressure, q_g is the constant pressure over a goaf area, q_c is the constant pressure over un-yielded coal seam (in-situ overburden pressure), q_{max} is the control factor of an overburden pressure peak, l_{ic} is the control factor of the rising overburden pressure, l_{dc} is the control factor of the decreased overburden pressure, l_y is the distance of yielded coal seam, and l_g is the half of goaf distance. For field practice, these parameters can be estimated or measured by the monitoring of rock pressure or using microseismic methods. An example is given in Fig. 3 to illustrate the use of Equation (1) in which q_g is 0.15 MPa, q_c is 8 MPa, q_{max} is 36 MPa, l_{ic} is 4, l_{dc} is 6, l_y is 10 m, l_g is 20 m (parameter value adopted from a case study illustrated by Zhang at al.[44]).
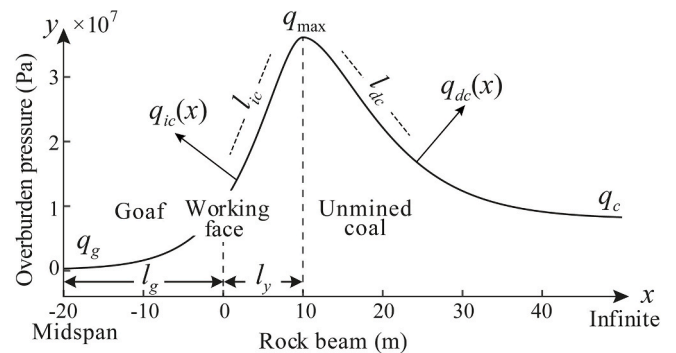

Fig. 3. Non-uniformly distributed overburden pressure.

2.3. Mechanical model of beam I-IV

Understanding the failure of roof strata and its control factors is to have the mechanical state of the proposed strata beam structure, which include the deflection (y), slope (θ), bending moment (M) and shear force (Q). However, as the discontinuity of the strata beam in terms of foundation conditions demonstrated in Fig. 2, the mechanical model needed to be structured piecewise from beam-I to beam-IV. To simplify the mathematical process, the superposition method for a beam over the elastic foundation was adopted to solve the equations for beam-IV. The mechanical models for strata and corresponding solving strategies are illustrated in Fig. 4.

2.3.1. Finite beam-I: over goaf

In this study, a typical longwall panel and an ideal overburden structure are adopted as the prototype . In this model, the immediate roof underneath the hard roof strata caved into pieces along with the excavation of a coal seam that cannot offer support resistance to the hard roof. Therefore, the support resistance of caved strata is neglected that means no foundation for the beam over goaf, the mechanical model is shown in Fig. 5.

As the strata beam over goaf area (not including beam over the face powered support) is an approximately symmetric structure, therefore the mechanical model of the strata beam can be achieved by half-length of it by providing support at $x = -l_g$, which restricts any rotation but allows vertical displacement. On the right side of beam-I, the boundary condition is represented by shear force Q_1 and bending moment M_1. Based on a basic beam theory, the mechanical state of beam-I can be expressed as

$$
\begin{cases}
y_I(x) = -\int \theta_I(x)dx + C_{I1} \\[2mm]
\theta_I(x) = -\dfrac{\int M_I(x)dx}{-EI} + C_{I2} \\[2mm]
M_I(x) = M_1 + Q_1(x - l_s) - \displaystyle\int_0^{x-l_s} q_{ic}(l_s+t)(x-l_s-t)dt \\[2mm]
Q_I(x) = -\dfrac{dM_I(x)}{dx} \\[2mm]
\end{cases}
\quad
\begin{aligned}
(-l_g \leq x \\ < -l_s)
\end{aligned}
\tag{2}
$$

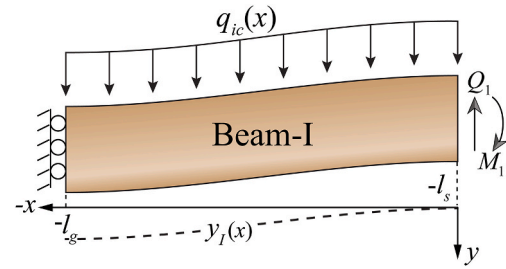**Fig. 4.** Application of the superposition method to solve the mechanical model of strata.

Fig. 5. Mechanical model of beam-I.

where C_{I1} and C_{I2} are constant of integration, $Q_1 = \int_{l_s}^{l_g} q_{ic}(x)dx$. As the domain of Equation (2) is negative, the negative sign should be introduced.

Looking at the boundary restrict at $x = -l_g$, a guided support end with 0 slopes, the boundary restrict can be expressed as $\theta_I(-l_g) = 0$. By substituting $\theta_I(-l_g) = 0$ into Equation (2), the integration constant C_{I2} is solved as

$$
C_{I2} = \theta_I(-l_g) + \frac{\int M_I(-l_g)dx}{-EI} = 0 + \frac{\int M_I(-l_g)dx}{-EI}
\tag{3}
$$

By substituting the rising overburden pressure function $q_{ic}(x)$, shear force Q_1 and C_{I2} into Equation (2), the deflection $y_I(x)$, slope $\theta_I(x)$, bending moment $M_I(x)$ and shear force $Q_I(x)$ of beam-I can be achieved with 2 unknowns, the integration constant C_{I1} and bending moment M_1.

2.3.2. Finite beam-II: over face powered support

The mechanical model of beam-II (Fig. 6) and beam-I are similar, except for the boundary conditions and the support resistance that act against the rising overburden pressure.

The support resistance $q_s(x)$ is directly offered by the residual immediate roof which is supported by the shield supports. If the canopy tip-to-end distance l_{t-f} is considered, the $q_s(x)$ is a redistribution of shield resistance $q_c(x)$. A study[60] suggested $q_c(x)$ can be simplified as a linear expression with the minimum q_{cmin} at the canopy tip and the maximum q_{cmax} at the canopy rear end. Assumption of the immediate roof over the excavated area is disconnected from one over coal seam (stress cannot be transferred to the front of working face). The correlation between $q_s(x)$ and $q_c(x)$ is shown in Fig. 7.

For simplification of expressions, the canopy tip-to-face distance is ignored in this study. Thus, $q_s(x) = q_c(x)$ can be simplified as a linear function with minimum value q_{smin} above working face and maximum value q_{smax} above canopy rear end.

$$
q_s(x) = q_{smin} + \frac{(q_{smax} - q_{smin})}{l_s}x \quad (-l_s \leq x < 0)
\tag{4}
$$

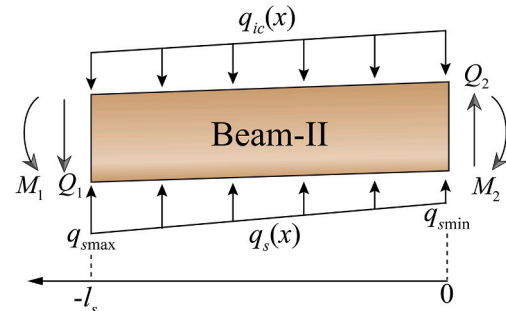By adding $q_s(x)$ as a reaction force of $q_{ic}(x)$, the function of beam-II can be written as
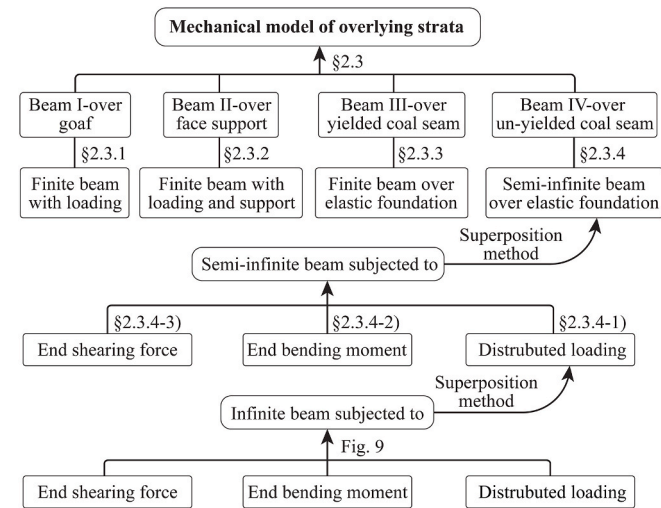
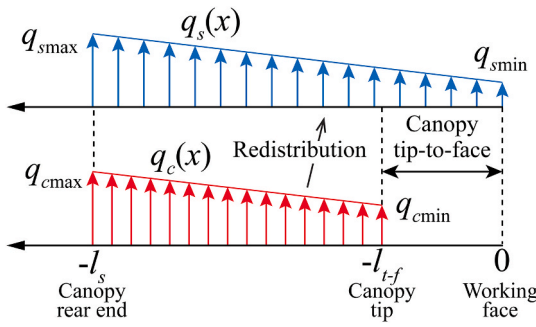**Fig. 6.** Mechanical model of beam-II.
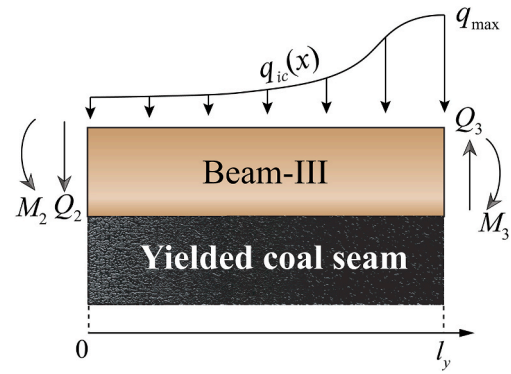
Fig. 7. Support resistance.

Fig. 8. Mechanical model of beam-III.

$$\begin{cases} y_{II}(x) = -\int \theta_{II}(x)dx + C_{II1} \\[2mm] \theta_{II}(x) = \dfrac{-\int M_{II}(x)dx}{-EI} + C_{II2} \\[2mm] M_{II}(x) = M_2 + Q_2 x - \int_0^x (q_{ic}(t) - q_s(t))(x-t)dt \\[2mm] Q_{II}(x) = -\dfrac{dM_{II}(x)}{dx} \end{cases} \quad (-l_s \le x < 0) \quad (5)$$

where C_{II1} and C_{II2} are constant of integration, $Q_2 = \int_0^{l_s} q_{ic}(x)dx - \int_0^{l_g} q_{ic}(x)dx$.

By substituting the rising overburden pressure $q_{ic}(x)$, the linear

yielded coal seam into account. In this part, a generalized form of an infinite beam on an elastic foundation is firstly adopted to develop the mechanical model without considering the yielded coal seam. The yielded coal seam is introduced in section 3. The comparison of yielded and un-yielded coal seam models is carried out in section 4.3. The mechanical model of beam-III is shown in Fig. 8.

Without considering the yielded coal seam, the mechanical model illustrated in Fig. 8 can be represented by the general solution of a finite beam on an elastic foundation, Equation (7). The general solution was developed by A.A.Umansky[61] and M.Heteneyi[51] as the method of initial parameters and the method of end conditioning, respectively.[62]

$$\begin{cases} y_{III}(x) = y_0 F_1(\lambda x) + \dfrac{1}{\lambda}\theta_0 F_2(\lambda x) - \dfrac{1}{\lambda^2}\dfrac{1}{EI}M_0 F_3(\lambda x) - \dfrac{1}{\lambda^3 EI}Q_0 F_4(\lambda x) + \dfrac{1}{\lambda^3 EI}\int_0^x q_{ic}(t)F_4[\lambda(x-t)]dt \\[2mm] \theta_{III}(x) = \dfrac{dy_{III}(x)}{dx} \\[2mm] M_{III}(x) = -EI\dfrac{d\theta_{III}(x)}{dx} \\[2mm] Q_{III}(x) = \dfrac{dM_{III}(x)}{dx} \end{cases} \quad (0 \le x < l_y) \quad (7)$$

support resistance $q_s(x)$ and shear force Q_2 at $x = 0$ into Equation (5), the deflection $y_{II}(x)$, slope $\theta_{II}(x)$, bending moment $M_{II}(x)$ and shear force $Q_{II}(x)$ of beam-II can be achieved with 3 unknowns, the integration constant C_{II1}, C_{II2}, and bending moment M_2.

Considering the continuity of strata beam-I and beam-II, boundary restricts are given as

$$\begin{cases} y_I(l_S) = y_{II}(l_S) \\ \theta_I(l_S) = \theta_{II}(l_S) \\ M_I(l_S) = M_{II}(l_S) \end{cases} \quad (6)$$

By substituting Equations (2) and (5) into Equation (6), the integration constant C_{II2}, C_{I1} and bending moment M_1 can be expressed by M_2 and C_{II1}, that is, only 2 unknowns for Equation (2) of beam-I and Equation (5) of beam-II.

2.3.3. Finite beam-III: over coal seam

Since the coal seam was excavated, the overburden pressure around the working face rapidly increases and exceeds the compressive strength of the coal seam near the working face. The yielded coal seam, near the working face, cannot offer full support resistance to overlying strata, the behaviour of overlying strata can be significantly influenced by the partially yielded coal seam.[57] Therefore, it is necessary to take the

where y_0, θ_0, M_0 and Q_0 are the quantities existing at the end $x = 0$, E and I are the plan strain modulus and the area moment of inertia of strata beam-III.

$$F_1(\lambda x) = \cosh \lambda x \cos \lambda x$$

$$F_2(\lambda x) = \frac{1}{2}(\cosh \lambda x \sin \lambda x + \sinh \lambda x \cos \lambda x)$$

$$F_3(\lambda x) = \frac{1}{2}\sinh \lambda x \sin \lambda x$$

$$F_4(\lambda x) = \frac{1}{4}(\cosh \lambda x \sin \lambda x - \sinh \lambda x \cos \lambda x)$$

where λ is the characteristic of the system

$$\lambda = \sqrt[4]{\frac{k}{4EI}}$$

where k is the modulus of the coal seam.

As the continuity of strata beam-II and beam-III, y_0, θ_0, M_0 and Q_0 can be expressed by substituting $x = 0$ into Equation (5). Therefore, Equation (7) of beam-III is derived with 2 unknowns, the integration constant C_{II1} and bending moment M_2.

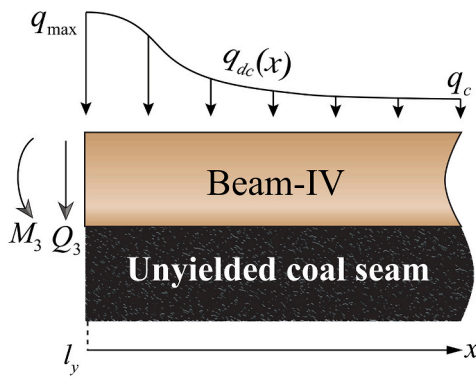Semi-infinite beam-IV: over coal seam.

Fig. 9. Mechanical model of beam-IV.

Fig. 10. Infinitely beam model.

In terms of the strata beam-IV over the un-yielded coal seam, the decreased overburden pressure $q_{dc}(x)$ from the peak at $x = l_y$ decreases continuously to in-situ overburden pressure q_c then extends unlimitedly to the $+x$ direction. The mechanical model of beam-IV can be simplified as a semi-infinite beam with non-uniformly distributed loading over an elastic foundation (Fig. 9).

For the proposed mechanical model of beam-IV, most studies aim to determine the integration constants from the prescribed end-condition of the elastic line. The main difficulty in applying the general solution to particular problems arises in the determination of the integration constants, which involves a considerable amount of work.[51]

To avoid the difficulties mentioned above, the method of super-position[63] is adopted for this study, the application of the superposition method is illustrated in Fig. 4. According to the method of superposition, for a beam over elastic foundation, the solution of beam-IV can be separated into 3 particular cases; 1) beam with free end subjected to distributed loading $q_{dc}(x)$, 2) beam with end bending moment M_3 and 3) beam with end shear force Q_3. Therefore, the solution of beam-IV can be expressed as the sum deflection of the 3 cases

$$\begin{cases} y_{IV}(x) = y_{IV\_DL}(x) + y_{IV\_BM}(x) + y_{IV\_SF}(x) \\ \theta_{IV}(x) = \dfrac{dy_{IV}(x)}{dx} \\ M_{IV}(x) = -EI\dfrac{d\theta_{IV}(x)}{dx} \qquad (l_y \leq x) \\ Q_{IV}(x) = \dfrac{dM_{IV}(x)}{dx} \end{cases} \quad (8)$$

where $y_{IV\_DL}(x)$, $y_{IV\_BM}(x)$ and $y_{IV\_SF}(x)$ is the deflection of beam-IV caused by distributed loading $q_{dc}(x)$, end bending moment M_3 and end shear force Q_3, respectively.

The calculation of $y_{IV\_DL}(x)$, $y_{IV\_BM}(x)$ and $y_{IV\_SF}(x)$ will be discussed in next paragraphs. For the concise form of expression, the following symbols are introduced:

$A(x) = e^{-\lambda x}(\cos \lambda x + \sin \lambda x)$
$B(x) = e^{-\lambda x} \sin \lambda x$
$C(x) = e^{-\lambda x}(\cos \lambda x - \sin \lambda x)$
$D(x) = e^{-\lambda x} \cos \lambda x$

1) Beam with free end subjected to distributed loading
For an infinitely beam with distributed loading $q(x)$ on an elastic foundation, Hetényi[51] suggested due to the loading $q(x)$, there is a bending moment M_A and a shear force Q_A at point A which maintain the continuity of beam at point A. Removal of M_A and Q_A will have the same significance for the right side of the beam as a removal of the whole portion to the left. Therefore, a semi-infinite beam can be achieved by applying bending moment M_{end} and shear force Q_{end} at point A to cause a bending moment $-M_A$ and shear force $-Q_A$ (Fig. 10).
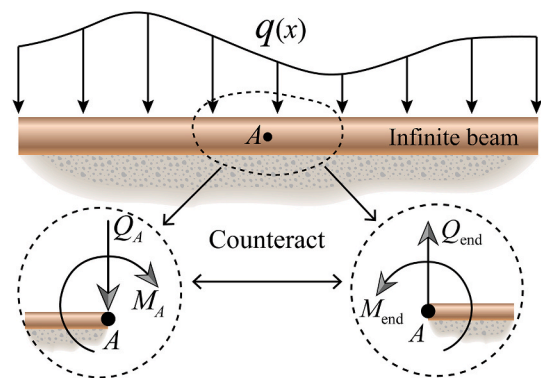
According to the method of superposition for a beam over elastic foundation, the solution of semi-infinite beam-IV subjected to distributed loading is achieved by the sum of 3 parts

$$y_{IV\_DL}(x) = y_{inf\_DL}(x) + y_{inf\_BM}(x) + y_{inf\_SF}(x) \quad (9)$$

where $y_{inf\_DL}(x)$, $y_{inf\_BM}(x)$ and $y_{inf\_SF}(x)$ is the deflection of an infinite beam subjected to distributed loading $q_{dc}(x)$, end bending moment M_{end} and end shear force Q_{end}.

Based on the knowledge of infinite beam on elastic foundation,[51] the solution of $y_{inf\_DL}(x)$ is given here directly

$$y_{inf\_DL}(x) = \frac{\lambda}{2k}\left[\int_0^{x-l_y} q_{dc}(t+l_y)A(x-l_y-t)dt + \int_{x-l_y}^{+\infty} q_{dc}(t+l_y)A(t-x+l_y)dt \right] \quad (10)$$

The solution of $y_{inf\_BM}(x)$ is

$$y_{inf\_BM}(x) = \frac{M_{end}\lambda^2}{k}B(x-l_y) \quad (11)$$

where the end bending moment $M_{end} = -\frac{2}{\lambda}\left(2\lambda M_{inf\_DL}(l_y) + Q_{inf\_DL}(l_y) \right)$.

The solution of $y_{inf\_SF}(x)$ is

$$y_{inf\_SF}(x) = \frac{Q_{end}\lambda}{2k}A(x-l_y) \quad (12)$$

where the end shear force $Q_{end} = 4\left(\lambda M_{inf\_DL}(l_y) + Q_{inf\_DL}(l_y) \right)$.

2) *Beam subjected to an end-bending moment*

The method illustrated above for the calculation of beam-IV subjected to distributed loading can also be used for deriving an expression for beam-IV subjected to end bending moment M_3. Here the bending moment M_A and shear force Q_A of the infinite beam at point A are $M_A = M_3$ and $Q_A = 0$. Therefore, the expression of the corresponding semi-infinite beam is

$$y_{IV\_BM}(x) = -\frac{2M_3\lambda^2}{k}C(x-l_y) \quad (13)$$

3) *Beam subjected to end shear force*

In the same manner, the formula can be derived for beam-IV subjected to end shear force. Here the bending moment M_A and shear force Q_A of the infinite beam at point A is $M_A = 0$ and $Q_A = Q_3$. Therefore, the expression of the corresponding semi-infinite beam is

$$y_{IV\_SF}(x) = \frac{2Q_3\lambda}{k}D(x - l_y) \qquad (14)$$

Since deflection expressions of beam-IV subjected to distributed loading $q_{dc}(x)$, bending moment M_3 and shear force Q_3 are available. By applying the method of superposition, the expressions of beam-IV, Equation (8), are achieved with 2 unknowns, the bending moment M_3 and shear force Q_3.

2.4. The solution of the elastic line equation

The expressions of beam-I, beam-II, beam-III and beam-IV have been introduced in the above section. However, there are 4 parameters, the integration constant C_{II1}, bending moment M_2, bending moment M_3 and shear force Q_3 that remain unknown. To solve these unknown parameters, the continuous boundary conditions at $x = l_y$, the intersection of beam-III and beam-IV, are adopted to get the following functions

$$\begin{cases} y_{IV}(x) = y_{III}(x) \\ \theta_{IV}(x) = \theta_{III}(x) \\ M_{IV}(x) = M_{III}(x) \\ Q_{IV}(x) = Q_{III}(x) \end{cases} \qquad (15)$$

According to the mechanical model and corresponding solving method illustrated above, the deflection, slope, bending moment and shear force of strata beam over coal seam before first weighting is achieved by solving Equation (15).

Overall, solutions for beam-I and beam-II are fundamental material mechanics. The solutions for beam-III are the general solution for the beam over elastic foundation problem. For beam-IV, the superposition method and the corresponding solutions are solved and given as a general solution.[51] Therefore, by using the superposition method, solving the mechanical model for overlying strata can be simplified without ardours mathematical computation.

3. Piecewise-defined function for strata over yielded coal seam

The general solution for strata beam over a coal seam is presented in the preceding sections. However, the yielded coal seam has not yet been considered in the model. Next, a piecewise-defined function approach is introduced to consider the yielded coal seam. The essence of the piecewise method is to divide beam-III into subsections and solve each of them by repeating the method illustrated in section 2.3.3 (finite beam over elastic foundation). Consequently, there is no new mechanical or mathematical models need to be introduced into the piecewise-defined method.

The modulus of a coal seam k is defined as the bearing pressure of the coal seam against the overloading that will produce a unit deflection of the foundation. The yielded state of a coal seam means the seam is losing the capacity to support the overloading. To some extent, a damped k may represent the yielded behaviour of a coal seam. Consequently, in this study, a variable modulus function $k(x)$ is proposed to represent a gradually yielded coal seam. As the blue dash line shown in Fig. 11, $k(x)$ is a linear function increases from $k(x) = k \cdot k_c$ at $x = 0$ to $k(x) = k$ at $x = l_y$, with modulus increment $= k(1 - k_c)$ and slope $= k(1 - k_c)/l_y$.

$$k(x) = k\left(k_c + \frac{1 - k_c}{l_y}x\right) \qquad (16)$$

where k_c (0,1) is the residual factor of foundation modulus. k_c ranges from 0 to 1 controls the modulus at $x = 0$ and the slope of the linear function. When $k_c = 0$, $k(x) = 0$ at $x = 0$ that means the coal seam is a totally yielded state at working face. When $k_c = 1$, $k(x) = k$ at $x = 0$ that means the coal seam is elastic state without any plastic damage at working face.

However, the function expression of k will pose difficulties in solving Equation (7). Thus, a piecewise-defined expression $k_n(x_n)$ is introduced to divide beam-III into n sections and keep modulus as a constant within the range of a single section. By substituting n for l_y in equation (16), the linear function $k(x)$ can be expressed as a piecewise function.

$$k_n(x_n) = k\left(k_c + \frac{1 - k_c}{n}x_n\right) \qquad (17)$$

where n is the number of sections that beam-III divided into, x_n is the nth section.

By adopting the piecewise-defined modulus $k_n(x_n)$, a stepped varying modulus of the foundation is proposed to represent the partially yielded coal seam (red lines in Fig. 11).

As shown in Fig. 11, the left boundary subjects to a bending moment M_2 and a shear force Q_2. For the sub-section beam k_1, substituting $x_n = 1$ into Equation (17) we get the modulus is $k\left(k_c + \frac{1 - k_c}{n}\right)$. Similarly with the finite beam on elastic foundation, the general expression of sub-section beam k_1 is obtained by using Equation (7) with 2 unknowns, the integration constant C_{II1} and bending moment M_2. By applying this process from the sub-section beam k_1 to k_n, the boundary conditions for sub-section beams can be transferred from the left side to the right side of beam-III, without introducing new unknown parameters. The bending moment and shear force of sub-section beam k_n to beam-IV are $M_{2.n}$ and $Q_{2.n}$, respectively, which is the M_3 and Q_3 shown in Fig. 9. When n is sufficiently large (usually $n \geq 5$), the solved curves would smoothen enough to represent beam-III over a linearly yielded coal seam, which can be found in the results of the following numerical studies. Another application of this piecewise-defined modulus and the proposed analytical model is to study the solid backfilling coal mining, which can be regarded as an elastic foundation with various foundation modulus.[64,65]

4. Model validation

The analytical solution for the whole strata beam has been derived. By using the proposed method, a parameter sensitivity analysis can be carried out to investigate the control factors for the failure of strata. Before applying this method to the numerical study, its validity should be verified by peer viewed results.

4.1. Validation testing

To verify the validity of the proposed analytical approach, validation testing is carried out. The calculated results of bending moment and shear force are compared with previous studies to showcase the accuracy of the proposed method. The input parameters are listed as "Validation testing" in Table 1.

Substituting the above parameters into proposed equations, the deflection, slope, bending moment and shear force of the given strata beam can be solved, corresponding results are shown in Fig. 12.

As shown in Fig. 12c and d, the validity of the application of the superposition method to solve the analytical model of overlying strata
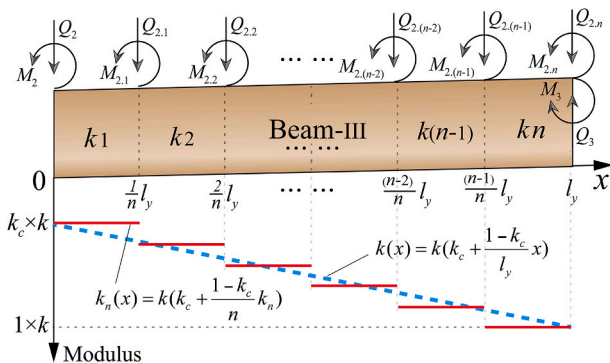

Fig. 11. Piecewise-defined modulus model of the yielded foundation.

Table 1
Model parameters setting.

Input parameter	Validation testing	Case study
Modulus of strata beam E (GPa)	25	31[a]
Unit width of strata beam b_w (m)	1	1
Thickness of strata beam b_h (m)	6	3.12
Half span of strata beam l_g (m)	20	10.2
Modulus of coal seam k (GPa)	0.8	2.1
Residual factor of coal seam modulus k_c	1	0.2
Yielded distance l_y (m)	0	8
Loading over goaf q_g (MPa)	0.15	0.3
Loading over un-yielded coal seam q_c (MPa)	8	6.75
Peak overburden pressure q_c (MPa)	9.68	13.5
Factor of the rising overburden pressure l_{ic} (m)	4	3
Factor of the decreased overburden pressure l_{dc} (m)	8	4
Roof support distance l_s (m)	5	4
Minimum support density q_{smin} (MPa)	1	0.3[b]
Maximum support density q_{smax} (MPa)	1.2	0.3[b]

[a] The lithology of strata rock in the case study is the sandstone (listed in Table 2), with uniaxial compressive strength 30.6 MPa, Poisson's ratio 0.24, Young's modulus 31.0 GPa and tensile strength 1.8 MPa.

[b] As the support density over the canopy tip and end are not monitored in field application, meanwhile, for the easy test the effect of various support distance and support density (see Table 4), we assume $q_{smin} = q_{smax} = 0.3$ MPa in the case study. A more accurate support resistance expression $q_s(x)$ is suggested to consider in the future study.

Source: The validation testing data are from a peer-reviewed study by Pan et al.[66] The case study data are based on the laboratory test, field survey and simplified assumption.

can be verified by consistent results. The possible tensile failure position is predictable by determining the maximum bending moment. In this case, the failure position is in front of the working face as its peak bending moment and is larger than the one at mid-span. The effect of support resistance can be represented by a sudden change in the shear force.

4.2. Strain energy density

Strain energy is the energy absorbed by the overlying strata during the retreat process.[67] Strain energy principles are widely used in determining the response of rock structures in both static and dynamic loads, such as rockburst and coal- and gas-outburst in underground longwall mining.[54,68] In practice, with the excavation, the strain energy will vary throughout the strata. For this reason, it is useful to introduce strain energy density, which is a measure of how much energy is stored in a small element throughout the strata.[69]

For a small element dx, the work is done by a moment $M(x)$ as it moves through an angle $d\theta$ to outline $M(x)d\theta/2$, where $d\theta = M(x)dx/EI$. The strain energy for the small element dx, the strain energy density is then

$$\frac{dU}{dx} = \frac{1}{2}M(x)d\theta = \frac{M^2(x)dx}{2EI} \tag{18}$$

Furthermore, a beam can also store energy due to its shear stress, which is usually much less than that due to flexural stresses provided if the beam is slender. Therefore, only strain energy density due to bending is considered in this study. As the bending moment, $M(x)$ is derived in the preceding sections, the strain energy density can be calculated. The strain energy density curve with initial conditions of Table 1 is shown in Fig. 13.

From the curve shown in Fig. 13, the energy accumulation area and the high-density area can be identified. The strain energy density of strata is another critical factor for dynamic disasters, such as rockburst, and coal- and gas-outbursts. Therefore, the strain energy density will be discussed in the following case studies.
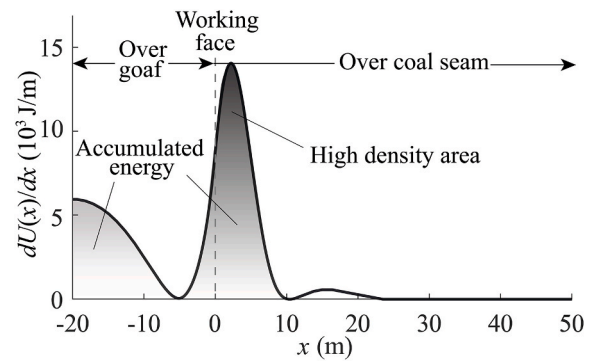

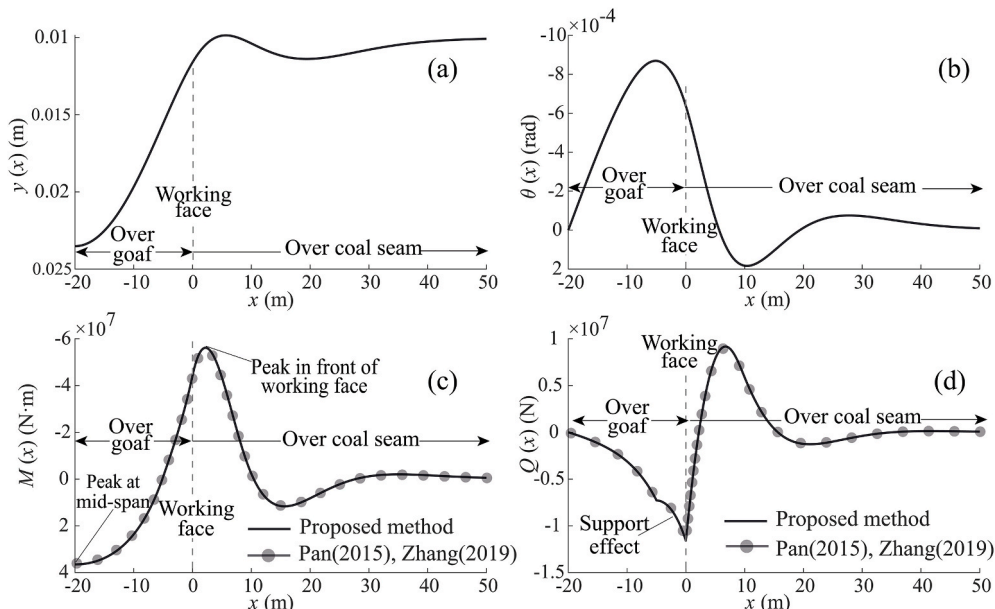**Fig. 13.** Strain energy density of strata with given initial conditions.

Fig. 12. Calculation results of strata beam with given initial conditions (a) deflection, (b) slope, (c) bending moment and (d) shear force.

4.3. Abutment pressure over coal seam

The abutment pressure refers to the redistribution of stresses around excavations. The calculation of abutment pressure has always been the most important topic in longwall design. Researches[53,70] have shown the magnitude and distribution of abutment pressure are closely related to the occurrence of dynamic disasters. According to Equation (19), the abutment pressure, i.e. the bearing pressure of the coal seam in front of the working face can be achieved.

$$p = ky \tag{19}$$

where k is the modulus of the coal seam, y is the deflection of strata.

The bearing pressure over the coal seam with the "validation testing" parameter setting is shown in Fig. 14.

In Fig. 14 the coal seam in front of the working face is considered as an un-yielded state. According to the deflection curve shown in Fig. 11a and Equation (19), the maximum bearing pressure is consequently located over the working face. However, such a result is not in accordance with the understanding of the abutment pressure distribution. Numerous studies[53,70,71] have suggested the peak stress is generally located in front of the working face. The counterintuitive bearing pressure in Fig. 14 suggests taking the un-yielded coal seam as the foundation cannot produce a practical result that is consistent with engineering practice.

In the following case studies, the partially yielded coal seam will be considered. Meanwhile, the abutment pressure results will be presented along with the deflection, slope, bending moment, shear force and strain energy density.

5. Case study

5.1. Introduction to the longwall site

An underground longwall panel in China (referred to "Longwall A" thereafter) had been selected for the case study. Longwall A is 203 m wide and 800 m long to mine no.17 coal seam. The thickness of the no.17 coal seam ranges from 0.8 to 1.25 m with an average of 1.05 m. The overburden depth 450 m. The lithology and mechanical properties for the roof strata of Longwall A are presented in Table 2. The main roof is the 3.12 m sandstone strata.

The ZY2600/6.5/16, 2-leg shield supports with 2600 KN maximum shield resistance were used for supporting the roof. Specification of
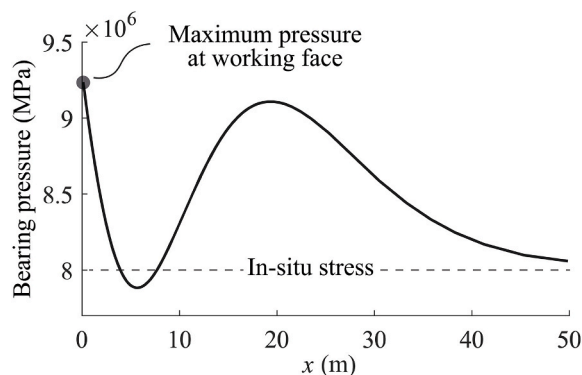

Fig. 14. Bearing pressure over coal seam.

Table 2
Mechanical properties of roof strata.

Strata	Thickness (m)	Density (kg/m^3)	Young's modulus (GPa)	Tensile strength (MPa)
...	440	1500	–	–
Sandstone	3.12	2480	31.0	1.8
Mudstone	1.75	2080	6.2	0.8
Coal seam	0.43	1380	1.2	0.2
Mudstone	0.90	1500	7.0	0.9
Mudstone	1.30	2080	6.2	0.8
Limestone	1.26	2500	32.0	3.0
No.17 Coal seam	1.05	1380	2.1	0.2

Source: The data obtained from geological survey and laboratory test.

Table 3
Technical data of shield support.

Type	ZY2600/6.5/16
Close height	650 mm
Extended height	1600 mm
Hydraulic leg	Double telescopic
Leg piston diameter	190 mm
Shield capacity	2600 kN
Shield density	0.36–0.44 MPa
Canopy length	3357 mm
Canopy width	1470 mm
Canopy ratio	2.86:1

Table 4
Tested control parameters.

Control Parameter		Value range
Residual factor of coal seam modulus k_c		[0, 0.1, …, 0.9, 1.0]
Yielded distance l_y (m)		[6, 7, 8, 9, 10]
Support capacity (kN) [0, 1200, 2400, 3600, 4800]	Support density q_{sd} (MPa)	[0, 0.3, 0.6, 0.9, 1.2] × 4m^2
	Support distance l_s (m)	[0, 2, 4, 6, 8] × 1 m × 0.6 MPa

shield support is as below:

Field monitored data suggested the first weighting distance of Longwall A is about 20.4 m. The input parameters of Longwall A for the proposed analytical model are listed as "Case study" in Table 1.

For engineering practice, strata control methods in longwall mining mainly include the adjustment of roof support scheme, destressing by artificially controlling the coal seam and overlying strata. For the proposed analytical model, the destressing can be achieved by adjusting the yielded degree k_c and yield distance l_y of the coal seam. The examination of the roof support scheme can be achieved by adjusting the support density q_{sd} and support distance l_s. To assess the influence of k_c, l_y, q_{sd} and l_s, a set of case studies are carried out by the parameter scheme listed in Table 3. The range of control parameters may not be practical; however, it is acceptable for the parameter sensitivity analysis.

Based on the initial parameter setting listed in Table 1, the deflection, slope, bending moment, shear force, strain energy density and bearing pressure over coal seam with corresponding tested parameter scheme listed in Table 3 are shown in Fig. 15 to Fig. 17.
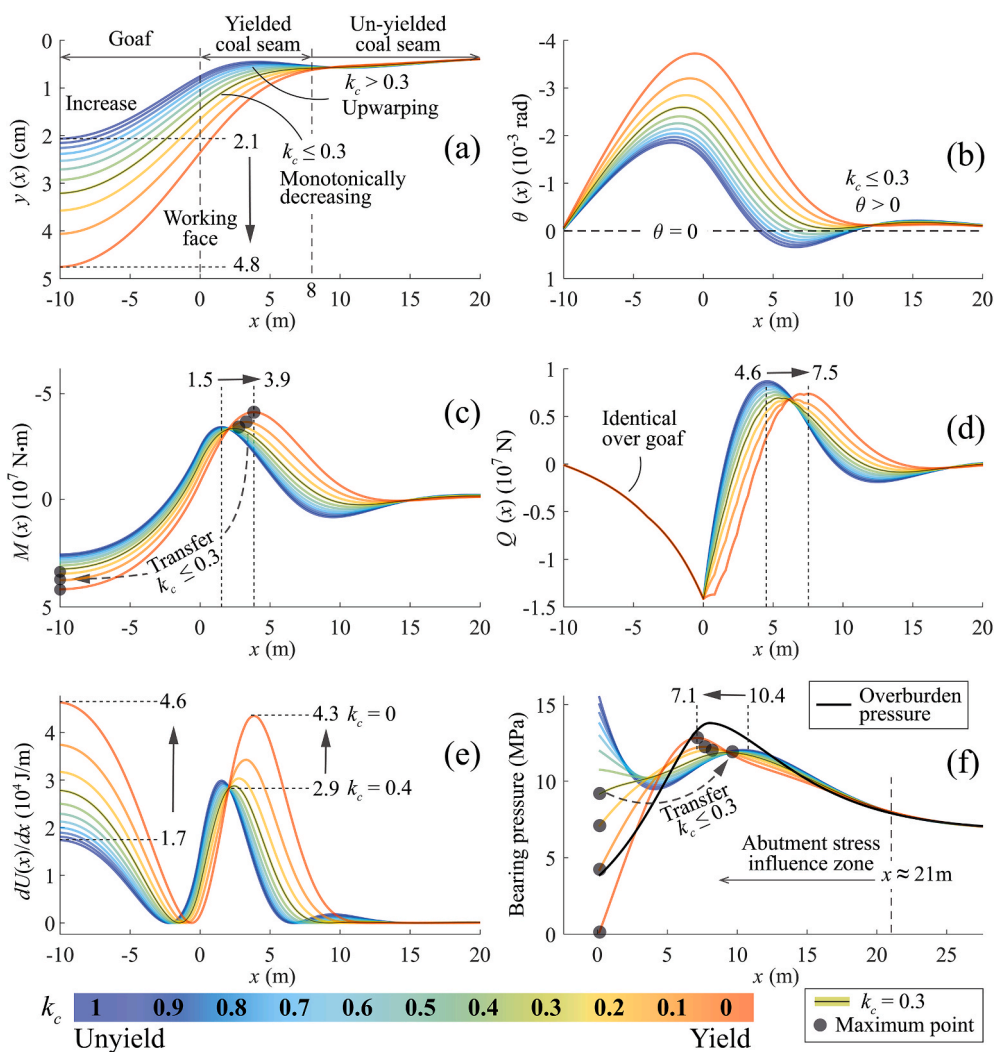
Fig. 15. Mechanical state of strata with various yield degrees of coal seam (a) deflection, (b) slope, (c) bending moment, (d) shear force, (e) strain energy density and (f) bearing pressure over coal seam.

5.2. Adjustment of coal seam

5.2.1. Yield degree of coal seam

The yield degree of the coal seam is achieved by adjusting the residual factor of coal seam modulus k_c. In this case, the tested k_c ranges from 0 to 1.0 with a 0.1 interval, the calculated results are shown in Fig. 15.

Fig. 15f suggests the bearing pressure over the working face can be adjusted by the yield degree of the coal seam. When $k_c \leq 0.3$, the maximum pressure, i.e. abutment peak, transfers from working face to the front, which is consistent with the most patterns observed in field practice. Therefore, curves of $k_c = 0.3$ were highlighted with a solid line. Discussions mainly focus on cases with $k_c \leq 0.3$. With the yield degree of coal seam from $k_c = 0.3$ increases to $k_c = 0$, the abutment peak rises from 11.9 MPa to 12.8 MPa, its location moves from $x = 10.4$ m to $x = 7.1$ m. Additionally, the bearing pressure reaches a balanced state with overburden pressure when $x > 21$ m (approximate). This indicates the influence distance of abutment pressure is about 21 m in front of the working face.

Fig. 15a suggests with the increase of the yield degree of the coal seam, the maximum deflection increases from 2.1 cm to 4.8 cm. Moreover, when $k_c > 0.3$, an up warping trend is detected over the yielded coal seam. However, for scenarios $k_c \leq 0.3$, the deflection curves present a monotonically decreasing trend thought out the whole strata (end at

midspan). This phenomenon can be verified by the slope curves shown in Fig. 15b. The slope is the first-order derivative of deflection with respect to x, the monotonicity of deflection can be interpreted as slope > 0 when $k_c \leq 0.3$.

In Fig. 15c, the maximum bending moment moves from over coal seam to over goaf when $k_c \leq 0.3$. This indicates the tensile failure of strata occurs over goaf when $k_c \leq 0.3$. This is an important change when studying the dynamic behaviour of strata as the corresponding energy release scenario can be significantly different from failure that occurs over coal seam. With the yield of the coal seam, the peak location moves from $x = 1.5$ m to $x = 3.9$ m.

Moreover, in Fig. 15d, shear force over goaf area keeps stable without any change, meanwhile, presents a decreasing trend with yield degree growth from $k_c = 1.0$ to $k_c = 0.1$, then bottom-up at $k_c = 0$. The peak location in front of the working face moves from $x = 4.6$ m to $x = 7.5$ m. In Fig. 15e, the strain energy density at midspan soars from 1.7×10^4 J/m to 4.6×10^4 J/m, whereas the peak over coal seam drops to 2.9×10^4 J/m at $k_c = 0.4$ then increases to 4.3×10^4 J/m. As the functional relation between bending moment and strain energy density is illustrated in Equation (18), the change of peak location of strain energy density is identical with the one of bending moment.

5.2.2. Yield distance of coal seam

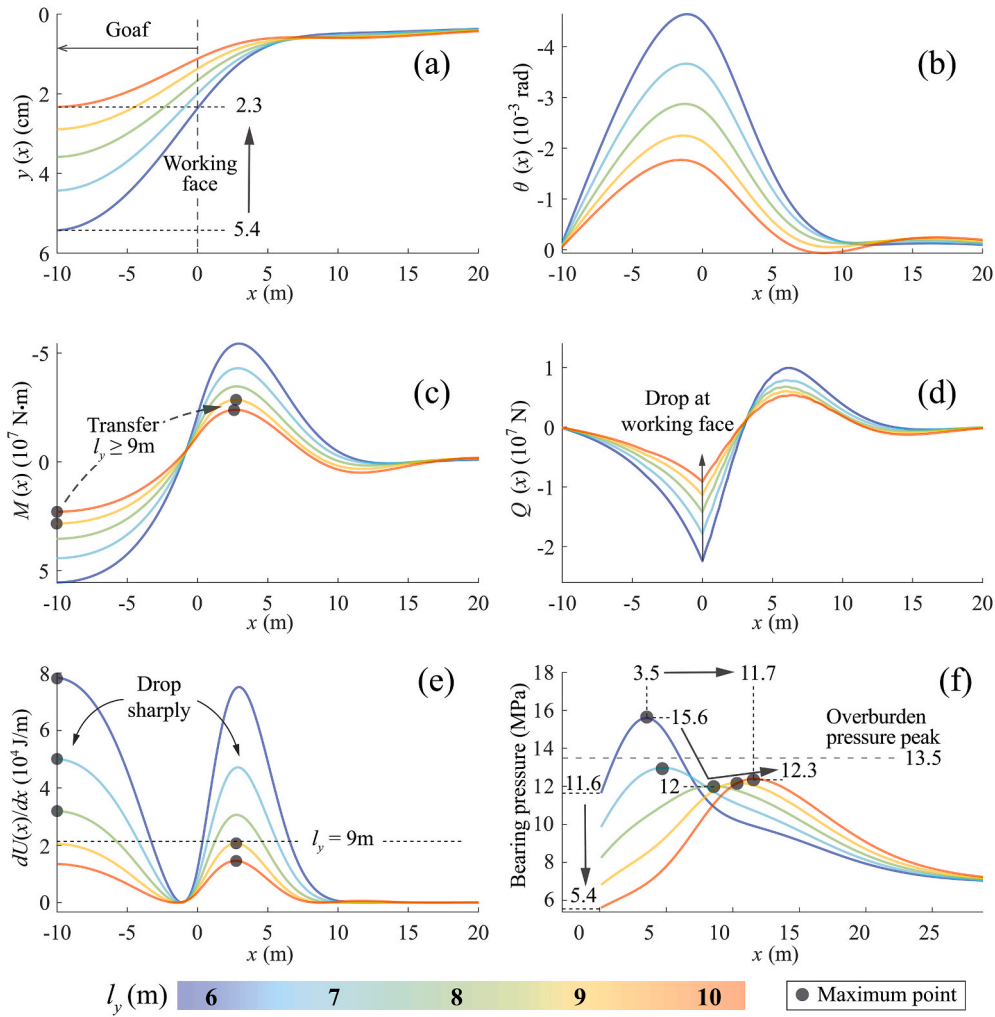In this section, the tested yield distance l_y ranges from 6 m to 10 m

Fig. 16. Mechanical state of strata with various yield distances of coal seam (a) deflection, (b) slope, (c) bending moment, (d) shear force, (e) strain energy density and (f) bearing pressure over coal seam.

with 1 m interval. The calculated results are shown in Fig. 16.

In Fig. 16f, with the yield distance increases from 6 m to 10 m, the pressure at the working face decreases steeply from 11.6 MPa to 5.4 MPa. The abutment peak drops from 15.6 MPa to 12.0 MPa then increases to 12.3 MPa. The peak location moves from $x = 3.5$ m to $x = 11.7$ m. Moreover, for cases of $l_y \geq 7$ m, all the abutment peaks are less than the peak overburden pressure 13.5 MPa. This suggests both the magnitude and the distribution of abutment can be significantly adjusted by controlling the yield distance of the coal seam.

Fig. 16a presents a counterintuitive trend that the deflection reduces from 5.4 cm to 2.3 cm while the yield distance increase from 6 m to 10 m. This phenomenon is caused by the distribution change of overburden pressure. As illustrated in section 2.2, the yield distance controls the peak of non-uniformly distributed overburden pressure. As the yield distance increases from 6 m to 10 m, the overburden pressure peak as well as the rising part (see $q_{ic}(x)$ in Fig. 3) move forward. As a result, the total pressure applied over the goaf area is reduced, thus, the deflection is reduced as well.

Fig. 16a–e suggest the deformation, bending moment, shear force and strain energy density of strata can be significantly reduced by increasing the yield distance of the coal seam. For instance, the maximum strain energy density both over midspan and over coal seam reduces from about 8×10^4 J/m to around 1.5×10^4 J/m. Moreover, the maximum bending moment transfers from over goaf to over coal seam when $l_y \geq 9$ m. As we stated in the last section, this means the failure

scenario could be very different and should be noticed when dynamic behaviour is considered.

5.3. Adjustment of roof support

The adjustment of the face support scheme mainly refers to the modification of support capacity, which includes two aspects: the support density and the support distance. In this section, the tested support capacity ranges from 0 to 4800 kN with a 1200 kN interval. Two schemes were designed to achieve the given support capacity: 1) 4 m support distance with support density increases from 0 to 1.2 MPa with 0.3 MPa interval, and 2) 0.6 MPa support density with support distance increases from 0 to 8 m with 2 m interval (Table 3).

The calculated results are shown in Fig. 17, in which Fig. 17(a1-a4) and Fig. 17(b1-b4) refers to the adjustment of support density and support distance, respectively. As strata deformation can be directly visualized by the deflection rather than the slope, therefore the slope results will not be presented here. Meanwhile, as the functional relation of Equation (18), the curve trend and peak location of bending moment can be demonstrated in strain energy density results, thus the bending moment results will not be presented as well.

In Fig. 17(a2) and (b2), the face support effect can be clearly observed. The shear force within the roof support range can be effectively reduced by both increase support density and distance. However, the shear force in front of the working face is barely influenced by
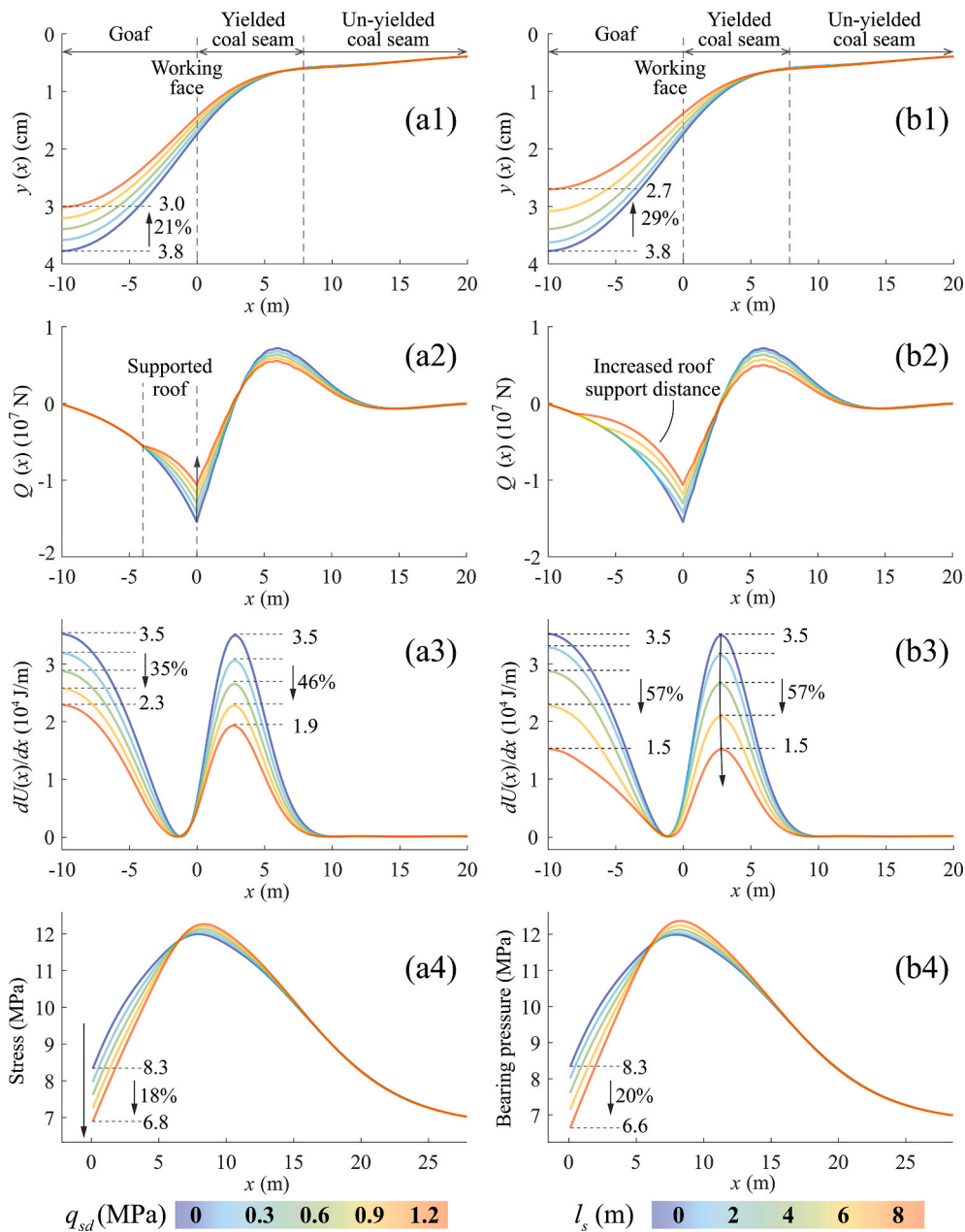
Fig. 17. Mechanical state of strata with various support density (*ai*) and support distance (*bi*). *i* = 1–4 refers to the (1) deflection, (2) shear force, (3) strain energy density and (4) bearing pressure over coal seam.

adjusting the support capacity. Both Fig. 17(a1) and (b1) suggest the deflection can be reduced by increasing support capacity. Furthermore, an increase of support distance reduces the deflection from 3.8 cm to 2.7 cm which is slightly better than adjustment of support density. As illustrated in Fig. 17(b3), an increase of support distance presents a similar control effect that reducing about 57% strain energy density both over goaf and in front of the working face. However, in Fig. 17(a3), an increase of support density presents a different control effect that reduces about 46% in front of working face and 35% over goaf. The bearing pressure in Fig. 17(a4) and (b4) decline similarly at the working face. The abutment peak shows an insignificant rising trend in front working face without obvious location change.

In practice, the adjustable support distance is limited, the canopy length of face support mainly ranges 4~6 m, the maximum support density is about 1.8 MPa.[72] The results may offer an approach to investigate strata control for (intermittent) cut-and-fill mining.
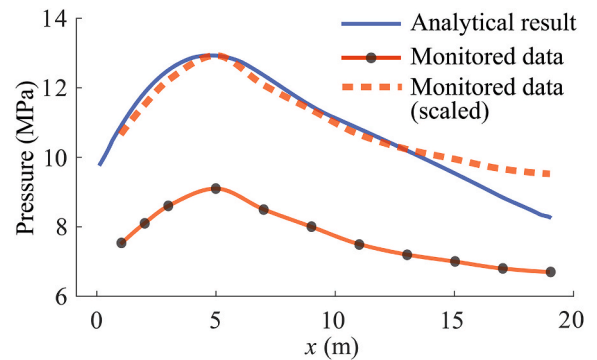

Fig. 18. Monitored props load and calculated bearing pressure.

6. Results and discussions

6.1. Calculated bearing pressure and field monitored results

The bearing pressure over the coal seam is a crucial reference when conducting a risk assessment for a longwall panel. Studies[38,52–54] have suggested bearing pressure as a static loading is the main contributor in a dynamic disaster. In practice, yielding is designated to control the majority of the overburden and abutment pressure transfer to the front of the working face. In this study, yielding refers to the increase in the yield distance and the yield degree. Among which increase yield distance effectively transfers the abutment peak away from the working face and reduces its magnitude, whereas increase the yield degree only reduces the bearing pressure within a small range from the working face. Adjustment of the support scheme shows a very limited control effect.

With regards to the ground pressure monitoring, borehole stress relief techniques, bore-hole pressure cells, bolt load cells, prop load cells, support leg pressure monitoring et al. have been extensively applied in field practice.[25,73] For Longwall A, single hydraulic props were set in the tailgate and headgate within about 20 m range in front of the working face with about 2 m interval. The loads of single hydraulic props in the head gate were monitored (red curve in Fig. 18). The monitored prop load presents a similar variation trend with the bearing pressure of 6 m yield distance case (blue curve in Figs. 18 and 16f). To compare the monitored and analytical data in a clear way, the measured props load is scaled to the maximum value of the analytical result (red dashed line in Fig. 18). The reason for the scaling of the monitored data is twofold. First, the props load is a behaviour of ground pressure redistribution rather than a direct measurement of ground pressure. Second, the monitored data could vary from monitoring equipment, installation methods and data interpretation methods. In practice, the yielded roof or floor, the setting distance of props, the inclination of props (load can be generated by axial strain or bending strain or a combination of both) and other factors could influence the monitored data. Thus, a practical way is to study the trend variation and stress increment that is correlated with the variation of coal seam bearing pressure. Scaling of the monitored props load is a way to highlight the correlation with the analytical result.

A similar trend of analytical and monitored results showcase the availability of the proposed method. On the other hand, it offers a possibility to estimate the yield degree and yield distance of coal seam by fitting the monitored stress distribution to an analytical case. In future study, borehole pressure cells monitoring is suggested to measure the vertical stress in front of the working face. Comparing with monitoring of prop load, borehole pressure cells monitor the vertical pressure in the coal seam directly which may reveal more strata behaviour when combined with the proposed analytical model.

6.2. The failure of strata

In most reported studies,[41,44,74,75] tensile failure is recognized as the main factor that controls the roof strata behaviour. According to the flexure formula,[76] the maximum tensile stress σ_{max} can be derived from the bending moment results.

$$\sigma_{max} = \frac{M_{max}c}{I} \qquad (20)$$

where M_{max} is the maximum bending moment, determined from the method proposed in section 2, I is the moment of inertia of the beam's cross-section, c is the distance from the neutral axis to the outermost point of the cross-section.

Based on the maximum tensile stress σ_{max} and the common statement of Hooke's law for isotropic elasticity,[77] the maximum tensile strain ε_1 can be derived.

$$\varepsilon_1 = [\sigma_1 - \nu(\sigma_2 + \sigma_3)]/E \qquad (21)$$

where σ_1 is the maximum tensile stress determined by Equation (20), σ_2 is $\nu(\sigma_1 + \sigma_3)$, σ_3 is the overloading $-q_{dc}(x)$ or $-q_{ic}(x)$, ν is Poisson's ratio.

According to Equations (20) and (21), both the maximum tensile stress and the maximum tensile strain have a linear functional relationship with a maximum bending moment. Consequently, the failure behaviour of strata can be interpreted by the magnitude and the position of a maximum bending moment.

The dynamic loading in a coal burst mainly refers to the sudden release of elastic strain energy stored in the strata. Equation (18) suggests the trend variation of strain energy density is correlated with the bending moment. Therefore, the magnitude and distribution of strain energy density are discussed in a similar manner to the bending moment.

4) The magnitude of bending moment and strain energy density

For controlling the magnitude of maximum bending moment, both adjustments of the support capacity and the yield distance of coal seam are viable approaches. Among which increase yield distance is the most practical and effective way to reduce the magnitude of bending moment as well as the strain energy density. For instance, yield distance increases from 5 m to 7 m, only 2 m difference, the maximum bending moment reduces over 50%, meanwhile, the maximum strain energy density reduces from 8×10^4 J/m to 3×10^4 J/m.

On the other hand, controlling of coal seam yield degree is very different, it is a non-monotonic relationship between the weakness degree of the coal seam and the magnitude of the maximum bending moment. With yielding, the maximum bending moment barely declined at first but increases rapidly over the unyielded level when reaching a very high yield degree.

In terms of the increase of coal seam yield distance, which is termed as the destressing or pre-conditioning in the mining industry, it has been applied in practice since the mid-20th century to limit the incidence and severity of rockburst around longwall face.[26,78] The widely used de-stressing techniques mainly refers to destress drilling, destress blasting and water infusion.[79–82] The latest researches attempted to achieve the de-stressing by microwave-induced fracturing apparatus,[83] coal face undercutting[84] and hybrid method.[85] It is hoped that this research will offer a new approach to evaluate the destress strategy and contribute to a deeper understanding of destress mechanism.

5) The location of the maximum bending moment

There are two bending moment peaks within the strata, one is located over the coal seam, another is over the goaf area. For most scenarios, the maximum is the peak in front of the working face. For the distribution of strain energy density, it is concentratedly distributed at the middle of the goaf area and in front of the working face over the yielded coal seam.

Concerning the location of bending moment peak in front of working face, only yielding of coal seam presents an obvious control effect, whereas adjustment of the support scheme and yield distance cannot change the location effectively. With yielding, the position of peak bending moment over coal seam keeps moving forward constantly.

An exceptional result is the peak bending moment over the goaf area turned to be the maximum one when the coal seam reaches $k_c \leq 0.3$ or $l_y \leq 8$ m. The phenomenon suggests both increase yield degree and reduces yield distance control the possible failure location of strata. Such a transfer of the maximum bending moment indicates the failure of the strata beam will occur over the goaf area firstly. As a result, the corresponding strain energy release scenario can be very different from the one failure in front of the working face.

6.3. Limitation of the proposed model

In the preceding sections, the proposed analytical method has been verified by comparing it to previous peer-reviewed studies. After that, the proposed method was adopted to investigate the control factors for the failure behaviour of overlying strata. As an improvement to previous studies, the yielded coal seam in front of the working face has been introduced into this method as an input parameter. The numerical case study also suggests there is a significant impact of the yielded coal seam on the mechanical behaviour of roof strata. However, in practice, the application of longwall mining is an extremely complex problem, some very key factors haven't yet been considered in the proposed analytical model. For instance, the retreat process and the plastic damage of strata. This is due to be considered in future work.

The proposed method is a static model that cannot take time-related factors into account. Numerous studies[86–88] have suggested the whole failure process of roof strata is a dynamic process that mainly refers to the crack initiation and propagation. In the future study, it is meaningful to explore the potential use of a time-related model, such as subcritical crack growth,[89,90] to realize the rock fracturing processes in the proposed model.

The numerical case studies carried out in section 4.3 are using a constant span distance to examine the mechanical behaviour of strata. In practice, the coal seam retreats at a certain speed, contributing to the span distance and its dynamic growth parameter. Therefore, the damage of strata is a dynamic process and as well as historical damage of rock should be considered when strata behaviour is evaluated under a given span distance.

From the view of energy evolution, there are three stages, strain energy accumulation, static dissipation and dynamic release.[52] By the proposed method, the strain energy accumulation can be calculated from the distribution of strain energy density. If above mentioned time-related behaviour can be added to the proposed model, then the full process of energy evolution is participated be achieved quantificationally.

7. Conclusion

The superposition method is adopted to solve the analytical model of hard roof strata before the first weighting in underground longwall mining. By using the proposed model, a considerable amount of mathematical work is averted, the partially yielded coal seam is achieved. The yielded coal seam is considered from yield degree and yield distance. A set of case studies were carried out to discuss roof control factors from the perspective of strata deflection, bending moment, strain energy density and coal seam bearing pressure. The following conclusions can be drawn.

1) For the tensile-dominated strata failure, the maximum bending moment is adopted to analyse the potential failure location. In most scenarios, the maximum bending moment locates in front of the working face. The location can be adjusted by both the yield degree and yield distance of the coal seam, whereas not sensitive to the face supports.
2) The strain energy density of strata can be significantly reduced by both increasing support capacity and increasing yield distance, rather than yield degree. With increasing yield degree, the strain energy density presents an unnoticeable decline trend at first, then increases rapidly to the highest level.
3) The distribution of bearing pressure over coal seam is greatly affected by both yield degree and yield distance of coal seam, whereas barely affected by roof support. A relatively high yield degree is essential to produce a rational bearing pressure distribution that conforms to the field measured pattern.

The superposition method offers a concise way to solve the analytical model of overlying strata. Based on this analytical model and the corresponding solving method, more factors, such as the damage of strata, the retreat scheme and geologic structures, are expected to be achieved in the future study.

Declaration of competing interest

The authors declare that they have no known competing financial interests or personal relationships that could have appeared to influence the work reported in this paper.

References

1 Majdi A, Hassani FP, Nasiri MY. Prediction of the height of destressed zone above the mined panel roof in longwall coal mining. *Int J Coal Geol*. 2012;98:62–72.
2 Wang W, Cheng Y, Wang H, et al. Fracture failure analysis of hard–thick sandstone roof and its controlling effect on gas emission in underground ultra-thick coal extraction. *Eng Fail Anal*. 2015;54:150–162.
3 Wang Jun, Ning Jianguo, Qiu Pengqi, Shang Yang, Shang Hefu. Microseismic monitoring and its precursory parameter of hard roof collapse in longwall faces: a case study. *Geomech Eng*. 2019;17(4):375–383.
4 Shen B, Duan Y, Luo X, et al. Monitoring and modelling stress state near major geological structures in an underground coal mine for coal burst assessment. *Int J Rock Mech Min Sci*. 2020;129:104294.
5 Donnelly LJ. A review of international cases of fault reactivation during mining subsidence and fluid abstraction. *Q J Eng Geol Hydrogeol*. 2009;42(1):73–94.
6 Sofianos AI. Analysis and design of an underground hard rock voussoir beam roof. *Int J Rock Mech Min Sci*. 1996;33(2):153–166.
7 Gray RE. Mining subsidence - past, present, future. *Int J Min Eng*. 1990;8(4):400–408.
8 Dumont G. *Des Affaisements du Sol Attributes a l'Exploitation Houillère*. German: Liège; 1871.
9 Fayol H. Note sur les mouvements de terrain provoqués par l'exploitation des mines. *Bulletin de la Société de l'Industrie Minérale*. 1885;2(24):805.
10 Jones OT, Davies EL. Pillar- and stall-working under a sandstone roof. *Trans Inst Mar Eng*. 1928;76(313).
11 Pugh WJ, Owen Thomas Jones. 1878-1967. Biogr mems fell R. *For Soc*. 1967;13 (1572):222–243.
12 Briggs H. *Mining Subsidence*. London: Edward Arnold; 1929.
13 Whittaker BN, Reddish DJ. *Subsidence: Occurrence, Prediction and Control*. Amsterdam: Elsevier; 1989.
14 King HJ, Whetton JT. Mechanics of mine subsidence. *Proc. European Congress on Ground Movement*. 1957:27–36.
15 Hackett P. An elastic analysis of rock movement caused by mining. *Trans Inst Mar Eng*. 1959;118:421–433.
16 Kapp WA. *Mine Subsidence and Strata Control in the Newcastle District of the Northern Coalfield New South Wales*. Doctoral thesis; 1984.
17 Boneva W. *A Study of Longwall Subsidence in the Appalachian Coalfield*. Masters Theses; 1982.
18 Berry DS. An elastic treatment of ground movement due to mining— I. Isotropic ground. *J Mech Phys Solid*. 1960;8(4):280–292.
19 Berry DS, Sales TW. An elastic treatment of ground movement due to mining—II. Transversely isotropic ground. *J Mech Phys Solid*. 1961;9(1):52–62.
20 Berry DS, Sales TW. An elastic treatment of ground movement due to mining—III three dimensional problem, transversely isotropic ground. *J Mech Phys Solid*. 1962;10 (1):73–83.
21 Salamon MDG. Elastic moduli of a stratified rock mass. *Int J Rock Mech Min Sci*. 1968; 5(6):519–527.
22 Salamon MDG. Two-dimensional treatment of problems arising from mining tabular deposits in isotropic or transversely isotropic ground. *Int J Rock Mech Min Sci*. 1968;5 (2):159–185.
23 Salamon MDG. An analogue solution for determining the elastic response of strata surrounding tabular mining excavations. *J S Afr Inst Min Metall*. 1964;65(2): 115–137.
24 Please CP, Mason DP, Khalique CM, et al. Fracturing of an Euler–Bernoulli beam in coal mine pillar extraction. *Int J Rock Mech Min Sci*. 2013;64:132–138.
25 Galvin JM. *Ground Engineering - Principles and Practices for Underground Coal Mining*. Cham: Springer International Publishing; 2016.
26 Brady BHG, Brown ET. *Rock Mechanics: For Underground Mining*. Dordrecht: Springer Netherlands; 2012.
27 Kratzsch H. *Mining Subsidence Engineering*. Berlin, Heidelberg: Springer Berlin Heidelberg; 1983.
28 Peng SS, ed. *Advances in Coal Mine Ground Control*. Duxford UK: Woodhead Publishing Elsevier; 2017.

29 Evans WH. The strength of undermined strata. *Trans Inst Min Metall*. 1941;(50): 475–532.

30 Beer G, Meek JL. Design curves for roofs and hangingwalls in bedded rock based on voussoir beam and plate solutions. *Trans Inst Min Metall*. 1982;18–22.

31 Diederichs MS, Kaiser PK. Stability of large excavations in laminated hard rock masses: the voussoir analogue revisited. *Int J Rock Mech Min Sci*. 1999;36(1):97–117.

32 Qian M, Shi P, Xu J. *Mining Pressure and Strata Control*. Xuzhou: China University of Mining and Technology Press; 2003.

33 Song Z. *Practical Ground Pressure Control*. Xuzhou: China University of Mining and Technology Press; 1998.

34 Sofianos AI. Discussion of the paper by M.S. Diederichs and P.K. Kaiser "Stability of large excavations in laminated hard rock masses: the voussoir analogue revisited". *Int J Rock Mech Min Sci*. 1999;36(7):991–993.

35 Shabanimashcool M, Li CC. Analytical approaches for studying the stability of laminated roof strata. *Int J Rock Mech Min Sci*. 2015;79(2):99–108.

36 Li Z, Xu J, Ju J, Zhu W, Xu J. The effects of the rotational speed of voussoir beam structures formed by key strata on the ground pressure of stopes. *Int J Rock Mech Min Sci*. 2018;108:67–79.

37 Newman D, Hutchinson AJ, Mason DP. Tensile fracture analysis of a thin Euler-Bernoulli beam and the transition to the voussoir model. *Int J Rock Mech Min Sci*. 2018;102:78–88.

38 Li Z, Dou L, Cai W, Wang G, Ding Y, Kong Y. Mechanical analysis of static stress within fault-pillars based on a voussoir beam structure. *Rock Mech Rock Eng*. 2016;49 (3):1097–1105.

39 Li Y. Analytical examination for the stability of a competent stratum and implications for longwall coal mining. *Energy Sci Eng*. 2019;7(2):469–477.

40 Jiang Y, Jiang J. The analytical solution of limit span for the clamped beam over elastic foundation. *Mech Eng*. 1991;13(1):55–57.

41 Pan Y, Wang Z, Li A. Analytic solutions of deflection, bending moment and energy change of tight roof of advanced working surface during initial fracturing. *Chin J Rock Mech Eng*. 2012;31(1):32–41.

42 Pan Y, Gu S, Wang Z. Influence of coal seam plastic zone on hard roof mechanical behaviour. *Chin J Rock Mech Eng*. 2015;34(12):2486–2499.

43 Yang S, Song G, Yang J. An analytical solution for the geometric broken characteristics of the overlying strata and its physical modeling study in longwall coal mining. *Arab J Geosci*. 2020;13(3):531.

44 Zhang Q, Peng C, Liu R, Jiang B, Lu M. Analytical solutions for the mechanical behaviors of a hard roof subjected to any form of front abutment pressures. *Tunn Undergr Space Technol*. 2019;85:128–139.

45 Froio D, Rizzi E. Analytical solution for the elastic bending of beams lying on a linearly variable Winkler support. *Int J Mech Sci*. 2017;128–129:680–694.

46 Zhang G, He F, Jiang L. Analytical analysis and field observation of break line in the main roof over the goaf edge of longwall coal mines. *Math Probl Eng*. 2016;2016(9): 1–11.

47 Huang P, Spearing AJS, Feng J, Jessu KV, Guo S. Effects of solid backfilling on overburden strata movement in shallow depth longwall coal mines in West China. *J Geophys Eng*. 2018;15(5):2194–2208.

48 Lu W, He C, Zhang X. Height of overburden fracture based on key strata theory in longwall face. *PloS One*. 2020;15(1), e0228264.

49 Wu L, Li M, He M. Force characteristic analysis of overlying stratum based on elastic foundation beam theory. *AMR (Adv Magn Reson)*. 2011;368–373:3167–3170.

50 Dinev D. Analytical solution of beam on elastic foundation by singularity functions. *Eng Mech*. 2012;19(6):381–392.

51 Hetényi M. *Beams on Elastic Foundation Theory with Applications in the Fields of Civil and Mechanical Engineering*. 1946.

52 Zhang C, Canbulat I, Hebblewhite B, Ward CR. Assessing coal burst phenomena in mining and insights into directions for future research. *Int J Coal Geol*. 2017;179: 28–44.

53 Dou L, Mu Z, Li Z, Cao A, Gong S. Research progress of monitoring, forecasting, and prevention of rockburst in underground coal mining in China. *Int J Coal Sci Technol*. 2014;1(3):278–288.

54 He H, Dou L, Gong S, He J, Zheng Y, Zhang X. Microseismic and electromagnetic coupling method for coal bump risk assessment based on dynamic static energy principles. *Saf Sci*. 2019;114:30–39.

55 Xu C, Yuan L, Cheng Y, Wang K, Zhou A, Shu L. Square-form structure failure model of mining-affected hard rock strata: theoretical derivation, application and verification. *Environ Earth Sci*. 2016;75(16):81.

56 Zhu W, Qi X, Ju J, Xu J. Mechanisms behind strong strata behaviour in high longwall mining face-ends under shallow covers. *J Geophys Eng*. 2019;16(3):559–570.

57 Wang C, Cao A, Zhang C, Canbulat I. A new method to assess coal burst risks using dynamic and static loading analysis. *Rock Mech Rock Eng*. 2020;53:1113–1128.

58 Li J, Huang Y, Zhang J, Li M, Qiao M, Wang F. The influences of key strata compound breakage on the overlying strata movement and strata pressure behavior in fully mechanized caving mining of shallow and extremely thick seams: a case study. *Adv Civ Eng*. 2019;2019:1–11.

59 Wilson AH. The stability of underground workings in the soft rocks of the Coal Measures. *Int J Min Eng*. 1983;1(2):91–187.

60 Rajwa S, Janoszek T, Prusek S. Influence of canopy ratio of powered roof support on longwall working stability - a case study. *J Min Sci Tech*. 2019;29(4):591–598.

61 Umansky AA. *Analysis of Beams on Elastic Foundation*. Leningrad: Central Research Institute of Auto-Transportation; 1933.

62 Tuma JJ, Alberti G. Static parameters of beams on elastic foundation. In: *Static Parameters of Beams on Elastic Foundation*. Springer; 1970:247–264.

63 Hetényi M. *Analysis of Bars on Elastic Foundation: Final Report of the 2nd International Congress for Bridge and Structural Engineering*. 1939. Berlin-Munich.

64 Huang Y, Li J, Ma D, Gao H, Guo Y, Ouyang S. Triaxial compression behaviour of gangue solid wastes under effects of particle size and confining pressure. *Sci Total Environ*. 2019;693:133607.

65 Li J, Huang Y, Chen Z, Zhang J, Jiang H, Zhang Y. Characterizations of macroscopic deformation and particle crushing of crushed gangue particle material under cyclic loading: in solid backfilling coal mining. *Powder Technol*. 2019;343:159–169.

66 Pan Y, Gu S, Yang G. Variation of internal force and rebound property of hard roof at initial stage of cracking. *Chin J Geotech Eng*. 2015;37(5):860–869.

67 Gere JM, Goodno BJ. *Mechanics of Materials*. eighth ed. Stamford CT: Cengage Learning; 2013.

68 Ning J, Wang J, Jiang J, Hu S, Jiang L, Liu X. Estimation of crack initiation and propagation thresholds of confined brittle coal specimens based on energy dissipation theory. *Rock Mech Rock Eng*. 2018;51(1):119–134.

69 Kelly PA. Mechanics lecture notes: an introduction to solid mechanics. Available at: http://homepages.engineering.auckland.ac.nz/~pkel015/SolidMechanicsBooks/index.html. Accessed February 1, 2020. accessed.

70 Liu H, Wang P, Liu Y, Dai J, Yang J. A new theoretical method for calculating front abutment stress during coal mining. *Energy Sci Eng*. 2020;8(3):836–848.

71 Zhu G-a, Dou L-m, Li Z-l, Cai W, Kong Y, Li J. Mining-induced stress changes and rock burst control in a variable-thickness coal seam. *Arab J Geosci*. 2016;9(5).

72 Wang J, Li Y. *Thick seam coal mining and its ground control. Advances in Coal Mine Ground Control*. Elsevier; 2017:379–407.

73 Sinha S, Walton G. Investigation of longwall headgate stress distribution with an emphasis on pillar behavior. *Int J Rock Mech Min Sci*. 2019;121(1):104049.

74 Jiang H, Cao S, Zhang Y, Wang C. Analytical solutions of hard roof's bending moment, deflection and energy under the front abutment pressure before periodic weighting. *J Min Sci Tech*. 2016;26(1):175–181.

75 Gu S, Jiang B, Pan Y, Liu Z. Bending moment characteristics of hard roof before first breaking of roof beam considering coal seam hardening. *Shock Vib*. 2018;2018(2): 1–22.

76 Hibbeler RC. *Mechanics of Materials*. Boston: Pearson; 2017.

77 Timoïsenko SP, Goodier JN. *Theory of Elasticity*. third ed. New York, NY: MacGraw-Hill; 1987.

78 Roux AJA, Leeman ER, Denkhaus HG. De-stressing a means of ameliorating rockburst conditions Part I the concept of de-stressing and the results obtained from its application. *J S Afr Inst Min Metall*. 1958;59(1):66–68.

79 Vennes I, Mitri H, Chinnasane DR, Yao M. Large-scale destress blasting for seismicity control in hard rock mines: a case study. *J Min Sci Tech*. 2020;30(2):141–149.

80 Konicek P, Soucek K, Stas L, Singh R. Long-hole destress blasting for rockburst control during deep underground coal mining. *Int J Rock Mech Min Sci*. 2013;61 (2–3):141–153.

81 Konicek P, Saharan MR, Mitri H. Destress blasting in coal mining - state-of-the-art review. *Procedia Eng*. 2011;26(2):179–194.

82 Tang BY. *Rockburst Control Using Destress Blasting. Doctoral Thesis*. Montreal: Canada; 2000.

83 Lu G, Feng X, Li Y, Zhang X. The microwave-induced fracturing of hard rock. *Rock Mech Rock Eng*. 2019;52(9):3017–3032.

84 Yardimci AG, Karakus M. A new protective destressing technique in underground hard coal mining. *Int J Rock Mech Min Sci*. 2020;130(5):104327.

85 Kang H, Jiang P, Wu Y, Gao F. A combined "ground support-rock modification-destressing" strategy for 1000-m deep roadways in extreme squeezing ground condition. *Int J Rock Mech Min Sci*. 2021;142(3-4):104746.

86 Kong X, Wang E, Li S, Lin H, Zhang Z, Ju Y. Dynamic mechanical characteristics and fracture mechanism of gas-bearing coal based on SHPB experiments. *Theor Appl Fract Mech*. 2020;105:102395.

87 Kong X, Wang E, He X, Zhao E, Zhao C. Mechanical characteristics and dynamic damage evolution mechanism of coal samples in compressive loading experiments. *Eng Fract Mech*. 2019;210:160–169.

88 Chen S, Guo W, Zhou H, Shen B, Liu J. Field investigation of long-term bearing capacity of strip coal pillars. *Int J Rock Mech Min Sci*. 2014;70:109–114.

89 Atkinson BK. *Fracture Mechanics of Rock*. second ed. London: Acad. Press; 1991.

90 Shen B, Stephansson O, Rinne M. *Modelling Rock Fracturing Processes: A Fracture Mechanics Approach Using FRACOD*. Dordrecht: Springer; 2014.